



Published in final edited form as:

Mol Cell. 2008 August 22; 31(4): 520–530. doi:10.1016/j.molcel.2008.08.004.

Genome-wide Analysis of the H3K4 Histone Demethylase RBP2 Reveals a Transcriptional Program Controlling Differentiation

Nuria Lopez-Bigas¹, Tomasz A. Kisiel¹, Dannielle C. DeWaal², Katie B. Holmes², Tom L. Volkert³, Sumeet Gupta³, Jennifer Love³, Heather L. Murray³, Richard A. Young³, and Elizaveta V. Benevolenskaya^{2,*}

¹Research Unit on Biomedical Informatics, Experimental and Health Science Department, Universitat Pompeu Fabra, Barcelona 08080, Spain

²Department of Biochemistry and Molecular Genetics, University of Illinois at Chicago, 900 South Ashland Avenue, Chicago, IL 60607, USA

³Whitehead Institute for Biomedical Research, 9 Cambridge Center, Cambridge, MA 02142, USA

SUMMARY

Retinoblastoma protein (pRB) mediates cell-cycle withdrawal and differentiation by interacting with a variety of proteins. RB-Binding Protein 2 (RBP2) has been shown to be a key effector. We sought to determine transcriptional regulation by RBP2 genome-wide by using location analysis and gene expression profiling experiments. We describe that RBP2 shows high correlation with the presence of H3K4me3 and its target genes are separated into two functionally distinct classes: differentiation-independent and differentiation-dependent genes. The former class is enriched by genes that encode mitochondrial proteins, while the latter is represented by cell-cycle genes. We demonstrate the role of RBP2 in mitochondrial biogenesis, which involves regulation of H3K4me3-modified nucleosomes. Analysis of expression changes upon RBP2 depletion depicted genes with a signature of differentiation control, analogous to the changes seen upon reintroduction of pRB. We conclude that, during differentiation, RBP2 exerts inhibitory effects on multiple genes through direct interaction with their promoters.

INTRODUCTION

Cell differentiation includes coordination of cell-cycle events with tissue-specific gene expression. Abnormal regulation of this coordination is a critical aspect of tumorigenesis. Multiple studies have shown that pRB controls differentiation by direct and indirect effects on transcription, although the underlying mechanisms are still unknown. pRB activity has been connected to the direct inhibition of the E2F transcription factors, which are required for activation of genes involved in DNA synthesis and cell-cycle progression (for review, see Dimova and Dyson, 2005). We previously showed that RBP2 is a critical pRB-interacting protein involved in differentiation control (Benevolenskaya et al., 2005).

©2008 Elsevier Inc.

*Correspondence: evb@uic.edu.

ACCESSION NUMBERS

Microarray data are available from <http://www.ncbi.nlm.nih.gov/geo/> under accession numbers GSE10635, GSE10636, GSE10560, and GSE9690.

SUPPLEMENTAL DATA

The Supplemental Data include Supplemental Experimental Procedures, seven data sets, ten figures, and five tables and can be found with this article online at <http://www.molecule.org/cgi/content/full/31/4/520/DC1/>.

Decreasing RBP2 protein levels by RNA inhibition (RNAi) phenocopied the reintroduction of pRB in *RB* null cells. We suggested that RBP2 (JARID1A/KDM5A) and pRB share common, although sometimes opposing, roles in the regulation of differentiation. RBP2 forms endogenous protein complexes with pRB, and its interactions with pRB mutants, including the mutants that do not interact with E2F1, track with their ability to promote differentiation. RBP2 and pRB act, at least in some cases, directly on the same target genes: two homeotic genes, *BRD2* and *BRD8*; and the *osteocalcin* gene, which is synthesized by osteoblasts.

A number of recent studies have demonstrated the role of RBP2 homologous proteins in the control of gene expression and cell fate determination (for review, see Benevolenskaya, 2007). In humans, RBP2 is the first identified member of the JARID1 family of proteins that contains three other proteins: JARID1B/KDM5B/PLU1, JARID1C/KDM5C/SMCX, and JARID1D/KDM5D/SMCY. Mammalian JARID1 proteins share with their orthologs from other organisms highly identical domains, namely JmjN, JmjC, ARID, C5HC2 zinc finger, and two to three PHD domains. Disclosing histone lysine demethylase activity in several JmjC proteins and in proteins containing a PHD domain prompted testing JARID1 protein binding to methylated histones. All four members of the JARID1 family were found to be demethylases specific to trimethylated lysine 4 of histone H3 (H3K4me3) (for review, see Cloos et al., 2008). Unlike the majority of histone-modifying enzymes, RBP2 binds DNA in a sequence-specific manner. The recent study involving NMR showed that RBP2 makes extensive contacts with DNA in its ARID domain, and this is essential for transcriptional regulation by RBP2 (Tu et al., 2008). Thus, binding to a specific cohort of genes would be a possible mechanism for RBP2 effects on differentiation. Investigation of plausible candidate genes have shown that, indeed, RBP2, JARID1B, and JARID1D are recruited to a number of developmental regulators (Christensen et al., 2007; Dey et al., 2008; Lee et al., 2007a).

Despite the increasing acknowledgment of the prominent role of JARID1 proteins in transcriptional regulation and cell differentiation, understanding of their transcriptional program is still limited. Here, we describe an integrative systems biology approach, involving genome-wide location analysis, gene expression profiling, and a number of computational analyses to unravel the molecular mechanisms of RBP2 regulation of differentiation. We show that RBP2 occupies promoters with trimethylated H3K4 and regulates two functionally distinct groups of genes: (1) differentiation-independent RBP2 target genes, which are involved in mitochondrial function and RNA/DNA metabolism, and (2) differentiation-dependent RBP2 target genes, which include cell-cycle genes. Recruitment of RBP2 to the promoter region of a key mitochondrial component results in demethylation of H3K4 at this promoter and its transcriptional repression. This suggests the mechanism for RBP2 effects on the mitochondrial network. Finally, we compared gene expression changes in *RB*^{-/-} cells with RBP2 knockdown by RNAi and cells with reintroduced pRB and revealed that RBP2-dependent genes read out the genes controlled by pRB.

RESULTS

Genome-wide Location of RBP2 during Differentiation

In order to better understand how RBP2 controls differentiation at the transcriptional level, we first identified the DNA targets of RBP2. Because RBP2 demethylates H3K4me3 (Christensen et al., 2007; Iwase et al., 2007; Klose et al., 2007) that occurs at transcription start sites (Bernstein et al., 2007), we reasoned that we would be able to detect RBP2 at proximal promoter regions. We investigated RBP2 occupancy in human promonocytic U937 cells and detected significant binding to the fragments corresponding to the proximal promoter regions but not to the coding regions of the genome (Figure 1A). U937 cells

differentiate to mature monocytes and macrophages in the presence of certain inducing agents, including TPA (Rovera et al., 1979). After treatment with TPA, the cells adhere to the surface, become growth arrested, show morphological features of monocytes, and develop increased expression of specific markers. The progressive and quantitative increase in expression of the surface antigen, CD11b, provides a measure of monocytic differentiation. At 96 hr of TPA treatment, almost all cells are nonproliferating, as evidenced by BrdU staining (Figure 1B). There is a ten-fold decrease in the number of cells in S phase and an increase in the G1 cell population. Although normally associated with cell-cycle arrest, commitment to differentiation can be uncoupled from this process. We followed CD11b expression and at 240 hr, found that ~60% of cells were positive for the CD11b monocytic marker. The role of pRB in the differentiation of U937 cells has been inferred; pRB and RBP2 associate in transcriptionally active chromatin at 27 hr after TPA treatment (Benevolenskaya et al., 2005; Bergh et al., 1997). To study occupancy by RBP2 as a function of differentiation, we performed location analysis in undifferentiated U937 cells (0 hr after TPA addition), at 27 hr, and at 96 hr after TPA addition (Figure 1C; see also Data Sets S1–S3 available online). In addition, we used SAOS-2 cells that are able to undergo differentiation-like changes upon reintroduction of pRB or knockdown of RBP2 representing an effective model system (Data Set S4).

The promoter microarray used in this study contains around 19K features. We found that RBP2 is bound to at least 267 target genes in any of the three studied conditions (Data Sets S1–S3). At 27 hr, 153 additional target promoters are revealed, while 92 are not bound by RBP2 at this stage, which might reflect the fact that RBP2 activity is modified by interaction with some other protein such as pRB. In addition, 75 more promoters are detected at 96 hr in expense of 103 cases of diminished binding. Also, RBP2 shows some cell-type-specific binding: 126 RBP2 targets (64% of targets in SAOS-2) are identical between cycling U937 and SAOS-2 cells (Data Sets S4 and S5). We found that, surprisingly, many RBP2 targets are nuclear genes encoding proteins localized to the mitochondrion, including mitochondrial ribosomal proteins. The number of mitochondrial target genes reached 72 genes (Data Set S6) when we considered proteins identified in a proteomics study (Mootha et al., 2003). The list of RBP2 targets also includes genes that are known to be coregulated with genes of mitochondrial function (e.g., *PPP2R5A*, *CRYZ*, *SUMO1P3*, *MLH1*) (Mootha et al., 2003). RBP2 target genes were next analyzed for enrichment of Gene Ontology (GO) terms using Z-score statistics (Figure 2A). This analysis showed that RBP2 targets are highly enriched for genes with the GO terms for cellular components: mitochondrion, ribonucleoprotein complex, and spliceosome complex and with the GO terms for biological processes: RNA metabolism (RNA splicing, mRNA processing, RNA helicases), nucleobase, nucleoside, nucleotide, and nucleic acid metabolism (which includes transcription factors, proteins involved in cell-cycle regulation, DNA repair, and subunits of RNA polymerases, hereafter referred as “DNA metabolism”) (Figures 2A, S1, and S2). When we study RBP2 target genes specific to particular time points, we observe a clear functional distinction of RBP2 targets specific for 96 hr. At 96 hr RBP2 starts to occupy genes involved in the M phase of the cell cycle, spindle formation, DNA replication, DNA recombination, and DNA repair. As an independent measure, we explored the presence of RBP2 target genes among two external data sets: genes encoding mitochondrial proteins determined by Calvo et al. (2006) and cell-cycle-regulated genes determined by Whitfield et al. (2002). Mitochondrial proteins are enriched among constitutive RBP2 target genes and RBP2 target genes specific to 0 hr and 27 hr (Figure 2B; Table S1). By contrast, cell-cycle-regulated genes are highly enriched among RBP2 target genes specific for 96 hr (p value $< 1E-16$; Table S1), when cells become arrested in G0/G1 phase as part of terminal differentiation. The highest overrepresentation of 96 hr-specific genes is observed for S phase genes. In summary, RBP2 occupies promoters of two classes of genes. The genes occupied by RBP2 in a differentiation-independent manner are common to different cell types and encode proteins involved in mitochondrial

activity and DNA/RNA metabolism. The genes occupied by RBP2 in a differentiation-dependent manner comprise cell-cycle genes.

The degree of overlap of RBP2 target genes in U937 and SAOS-2 cells is very robust (Data Set S5), which is consistent with our previous data that RBP2 plays a role in pRB-mediated differentiation in very different cell types. We asked if RBP2 and pRB regulate common genes. Indeed, very significant overlap is evident between gene expression changes in the *RB*^{-/-} cells with RBP2 knockdown by RNAi and the cells with reintroduced pRB (p value = 1.1E-122) (Figure 2C; Table S2). This is consistent with our observation that the depletion for RBP2 phenocopies reintroduction of pRB in *RB*^{-/-} cells, thus supporting the evidence that RBP2 is downstream of pRB in the pathway (Benevolenskaya et al., 2005). It is particularly interesting that the genes with changed expression in cells with reintroduced pRB or depleted for RBP2 are the most overrepresented in the GO term extracellular region (Figure 2A).

Correlation between H3K4me3 and RBP2 Target Genes

RBP2 contains up to three PHD domains, which in other proteins have recently been shown to be H3K4me2/3 binding motifs (Taverna et al., 2007). Also, H3K4me3 modified nucleosomes associate near promoter regions. In order to examine how RBP2 relates to the presence of H3K4me3, we performed ChIP-on-chip analysis of H3K4me3 in U937 cells (0 hr) and compared the results to the RBP2 data. We observe that about half of the RBP2 targets are also positive for H3K4me3 (Figure 3), which represents a very high proportion (p value = 4.9 E-145). This suggests that the recognition of H3K4me3 may be important for RBP2 binding.

Nucleosomes with H3K4me3 are known to positively correlate with actively transcribed genes (Bernstein et al., 2002; Guenther et al., 2007). We analyzed the level of expression of genes with H3K4me3 modification in U937 cells, finding that, as expected, it is significantly higher for genes with trimethylated H3K4 (Table S3). Next, we explored whether RBP2 target genes experience other hallmarks of transcriptional activity in ES cells by comparing to recently published data (Guenther et al., 2007; Mikkelsen et al., 2007). We found that RBP2 target genes exhibit enrichment for transcriptional initiation and elongation marks, while are underrepresented among the “bivalent” H3K4me3/H3K27me3 promoters (Figure S3).

Promoter Sequence Analysis for Transcription Factor Binding Sites

In order to study which other factors might contribute to RBP2 recruitment to its target promoters, we performed a transcription factor binding site study. We searched promoters that were constitutively or differentially occupied by RBP2 during differentiation using position weight matrices (PWMs) of known DNA-binding sites of transcription factors in TRANSFAC (Matys et al., 2003) and compared their occurrence in all the genes represented on our microarray. RBP2 has been shown to interact with a number of proteins: pRB family proteins, TATA-binding protein (TBP), and a repressor of erythroid development, Rhombotin-2 (Fattaey et al., 1993; Kim et al., 1994; Mao et al., 1997). Although one could expect TBP-binding sites in RBP2-targeted promoter regions, interestingly, we also found high overrepresentation of pRB/E2F and Rhombotin-2 binding sites, which provides a validation of our analysis (Figure 3; Table S4). Consistent with the existence of a specific class of targets in differentiated cells (Figure 2), RBP2 targets at 96 hr include a substantial portion of E2F-responsive genes (PWMs of Rb:E2F-1: DP-1, E2F1, and E2F-1 in Figure 3). Comparison to experimental data on E2F4 location by other groups (Balciunaite et al., 2005; Boyer et al., 2005; Hollenhorst et al., 2007; Mikkelsen et al., 2007) confirmed this result (Figures 3, S3, and S4, and data not shown). RBP2 targets at 96 hr also contain binding sites

for the paired box protein Pax-6. Besides the differentiation-dependent binding, our analysis demonstrated ubiquitous RBP2 binding to promoters with binding sites for ETS-1 and ELK-1, the ETS DNA binding domain proteins that are required for the activation of many different genes in immature hematopoietic and mesenchymal cells. Analysis of genome-wide data for the ETS family (Hollenhorst et al., 2007) also showed high correlation with RBP2 occupancy (Figure 3). In conclusion, RBP2 forms a complex or is in close proximity to the pRB repressor complex on cell-cycle genes or to the transcriptional regulators responsive to specific developmental cues.

Correlation of Gene Expression with RBP2 Occupancy

The H3K4 demethylase activity of RBP2 indicates a repressive function. Gene expression profiling experiments performed in parallel with location analysis showed that only a subset of RBP2 target genes are differentially expressed during analyzed time points (Figure S5). We performed real-time PCR for a number of cell-cycle genes that are RBP2 targets specific for differentiated cells (Figure 4A and data not shown). This analysis demonstrated that the expression of these genes, for example *NUSAPI* and *PCNA*, drops by two- to three-fold when RBP2 is recruited to their promoters (96 hr) and ceases completely by 240 hr. Since the tested cell-cycle genes showed correlation between recruitment of RBP2 and decreased activity, we asked whether there are some gene expression changes that are characteristic for the whole group of targets at 96 hr. As a measure of their transcriptional activity, we used gene expression profiling data to evaluate relative probe intensity for this group compared to the rest of the genes. First, we found that at 96 hr RBP2 is preferentially recruited to the genes that are actively transcribed (Figure S6; Table S5). The proportion of highly active genes that are RBP2 targets is higher than the proportion of genes with similar activity that demonstrate enrichment for H3K4me3 (Figure S6). Second, a significant number of target genes specific for 96 hr have lower fold change values at 96 than at 27 hr, which means that there is a tendency that these genes (targets specific at 96 hr) are downregulated from 27 to 96 hr (p value < 0.009, Figure 4B). If RBP2 is involved in repression of its targets at 96 hr, then its forced expression will cause further reduction in the target gene activity. We noted that indeed overexpression of RBP2 results in a drop in the *PCNA* and *NUSAPI* expression levels that we observe at 96 hr (Figure 4C). Therefore, RBP2 is recruited to preferentially active genes during differentiation. These differentiation-dependent RBP2 target genes are getting repressed upon RBP2 binding.

Next, we asked whether the expression of RBP2 target genes shows any tissue specificity by examining Gene Atlas expression data for 79 human mature tissues and cell lines (Su et al., 2004). We first showed that genes with changed expression during the TPA treatment are preferentially expressed in hematopoietic tissues, as expected (Figure S7). In contrast, RBP2 target genes are preferentially expressed in six leukemia and lymphoma derived cell lines and five immunohistochemically defined blood samples: CD105+ and CD34+ subsets, and in B- and Natural Killer (NK) cells (Figure S7). The rest of the tissues had RBP2 target gene expression levels at least two-fold less.

Mechanisms of RBP2 Effects on Mitochondria

Since RBP2 is bound to promoter regions of multiple genes encoding components of mitochondria, we reasoned that it might regulate their expression levels. If so, then changes in RBP2 protein levels can affect mitochondrial function. We treated SAOS-2 cells with siRNA to RBP2 or overexpressed HA-tagged versions of RBP2 in these cells and analyzed mitochondria by immunofluorescence. Control cells transfected with a scrambled version of RBP2 siRNA or vector show a range of mitochondrial morphologies. The major morphological class, representing >80% of cells, can be characterized as tubules (Figures 5A and 5B). Surprisingly, cells with RBP2 knockdown had far-reaching tubules that formed

very dense mitochondrial networks (Figure 5A). The long tubule phenotype was also evident in SAOS-2 cells treated with two other RBP2 siRNAs but not with any of control siRNAs (Figures S8A and S8B). In contrast, cells overexpressing RBP2 displayed short mitochondria (rods), with the cells producing high RBP2 levels displaying dramatically fragmented mitochondria (spheres). Overexpression of the RBP2 mutant with compromised histone demethylation activity led to a much less degree of fragmentation and the appearance of normal tubules. Depletion of RBP2 in SAOS-2 cells results in cell-cycle arrest as evident, for example, by a drastic decrease in the Ki67 marker (Benevolenskaya et al., 2005). Consistent with these data, cells lacking RBP2 by siRNA are primarily Ki67 negative (Figure S8C). To ask if the long tubule phenotype is due to cell-cycle arrest, we performed double immunostaining for Ki67 and COX4. We first found an increased proportion of cells exhibiting long tubule morphology among Ki67 negative cells that were transfected with RBP2 siRNA but not in control cells, suggesting that the morphology is RBP2 dependent (Figures S8D and S8E). We next arrested cells by contact inhibition or by inhibition of cyclin-dependent kinases (CDKs). Contact inhibition or overexpression of the CDK inhibitor p21 efficiently blocked cell proliferation, as judged by Ki67 marker, but failed to result in the appearance of long tubules (Figures S8F and S8G), suggesting that formation of networks of interconnected mitochondria is not a characteristic of cell-cycle arrest. Since manipulation of RBP2 levels produced an interesting mitochondrial morphology phenotype, we next asked if the redox potential and/or mitochondrial fusion changes in these cells. By using RedoxSensor in live cells, we found that, while the whole expanded mitochondrial network is stained in cells with RBP2 knockdown, mitochondrial staining, and thus redox potential, is limited in cells with RBP2 overexpression (Figure 5A). Mitochondrial morphology is continuously changed by fusion and division. Among the best known proteins involved in mitochondrial dynamics are mitofusins, transmembrane GTPases that directly mediate mitochondrial outer membrane fusion. MFN2 colocalizes with the COX4 protein (Rojo et al., 2002), which we used as a mitochondrial marker. In *Mfn2* mouse knockout cells mitochondria undergo fusion events less frequently, which results in spherical morphology of mitochondria (Chen et al., 2003). Knockdown of MFN2 by siRNA in SAOS-2 cells led to the appearance of round mitochondria localized in patches around nuclei (Figure 5A). The phenotype in cells with MFN2 siRNA was quite different from the phenotype in cells overexpressing RBP2, suggesting that RBP2 also affects other mitochondrial components or functions. Since RBP2 knockdown augments appearance of filamentous mitochondria and RBP2 overexpression leads to fragmented mitochondria, we reasoned that RBP2 either inhibits fusion, and thus might repress *MFN2* gene activity, or promotes division. To test requirement of RBP2 for MFN2 repression, we performed qRT-PCR analysis in SAOS-2 cells with RBP2 knockdown or overexpression (Figure 5C). We noticed an increase in *MFN2* mRNA levels in cells treated with RBP2 siRNA, while RBP2 overexpression decreased the *MFN2* mRNA levels. Taking into account that expression of the RBP2 mutant does not cause severe mitochondrial segregation like the wild-type RBP2 (Figure 5A), one would suggest that RBP2 suppresses *MFN2* gene by H3K4 demethylation. To test this, we examined the H3K4me3 abundance at the *MFN2* promoter in SAOS-2 cells treated with RBP2 siRNA. These cells had high levels of H3K4me3 at the promoter (Figure 5D), while comparison of the total H3 levels showed no increase (data not shown). Our ChIP-on-chip data showed that RBP2 is bound to the promoter region of the *MFN2* gene at 27 hr in U937 cells (p value = 0.00018). Remarkably, *MFN2* gene expression level changes after TPA treatment of U937 cells, with a dramatic decrease at the 18–27 hr interval (Figures 5E and S9). RBP2 recruitment to the *MFN2* promoter correlates with the decrease in the promoter activity and with a significant decrease in the H3K4me3 present at the *MFN2* promoter (Figures 5F and 5G). This leads to the assumption that the *MFN2* expression level can be regulated by H3K4 demethylation. We conclude that RBP2 regulation of mitochondrial components includes demethylation of the nucleosomes with H3K4me3.

DISCUSSION

By using a combination of approaches that complement location analysis, we found several lines of evidence that RBP2, like pRB, plays a role in differentiation. We identified two functionally distinct classes of genes that are occupied by RBP2 in differentiation-dependent and -independent manners, which offer insights into the regulation of cell-cycle genes and mitochondria biogenesis in differentiating cells. The differentiation-dependent RBP2 binding correlates with high gene activity and is aimed at the cell-cycle genes that are destined for repression. RBP2 also regulates components of the mitochondrion and is necessary for normal mitochondrial function. Repression by RBP2 involves the direct effects on H3K4 methylation levels. Analysis of RBP2 target promoters and the distribution of nucleosomes with H3K4me3 modification suggest that RBP2 recognizes modules in the promoter regions in addition to H3K4me3. Our promoter sequence analysis indicates that these modules may be other transcription factors, including E2F and pRB family members. Consistent with the idea that RBP2 controls pRB-dependent genes, the correlation in the expression changes after depletion of RBP2 and reintroduction of pRB is highly significant and reflects the restored ability of cells to produce extracellular proteins and proteins with a function in development.

We provide evidence for changes in the expression of genes that are differentially occupied by RBP2 during differentiation (Figure 6). In growth-arrested cells that start to express markers of differentiation, such as U937 cells at 96 hr under TPA treatment, RBP2 is recruited to cell-cycle genes. These genes, however, are initially highly expressed until a later point in differentiation progression, when their two- to three-fold decrease in expression coincides with recruitment of RBP2. The shift to the actively transcribed genes at 96 hr is consistent with the idea that RBP2 appears in a fraction of active chromatin after the induction of differentiation (Benevolenskaya et al., 2005). RBP2 repression of E2F targets might be generally assisted by E2F4, p107, and p130 complexes to achieve full repression. RBP2 interacts with p130 in a yeast two-hybrid system (E.V.B., unpublished data), suggesting that it may not only be recruited to the same promoters as RBP2, but also be a part of its protein complexes. While Pax-9 has been identified in a yeast two-hybrid screen with PLU1 (Tan et al., 2003), we found overrepresentation of Pax-6 binding sites in RBP2 targets. Analogous to the PLU1 action, RBP2 might act as a Pax protein corepressor in differentiated cells. Consistent with this notion, it may be possible that RBP2 needs additional factors to be present at the promoter for repression to occur. In support of this, there is preferential recruitment of RBP2 in differentiated cells to highly active promoters that possess particular chromatin configuration and promoter motifs. Further, because at least half of its “constitutive” RBP2 target genes retain nucleosomes with H3K4me3 and their expression remains at average level, it is possible that RBP2 is present in an active form capable of demethylation when unbound to promoter, which then resolves H3K4 methylation upon binding, or that, in the promoter-bound form, RBP2 demethylation activity may be antagonized by histone H3K4 methyltransferases. In addition, DNA contact RBP2 mutants that retain histone demethylase activity show reduced activation of RBP2-dependent *BRD2* promoter (Tu et al., 2008), supporting the idea that DNA binding contributes to RBP2 recruitment and demethylation of specific genes.

Analysis of human cells and tissues showed that RBP2 is bound to genes where high expression is a feature of pluripotency, CD105+ and CD34+ cells. CD105 expression is a putative marker for mesenchymal stem cells (MSCs). CD34+ subset is enriched for hematopoietic stem cells (HSCs) and early progenitor cells. Many RBP2 targets encode proteins involved in DNA metabolism, including various transcriptional regulators. Their transcriptional repression versus activation in MSCs and HSCs may be important in programming differentiation. These conclusions can provide an explanation for the

abnormalities in *RBP2*^{-/-} mice, which demonstrate increased entry into G1 phase and decreased apoptosis in HSC, and an increased number of myeloid progenitor cells in S/G2/M (Klose et al., 2007). *RBP2* target genes are also overrepresented among genes preferentially expressed in human leukemia and lymphoma. *RBP2* has recently been shown to be involved in a translocation in a patient with acute myeloid leukemia (van Zutven et al., 2006). When taken together, these data suggest that *RBP2* has a distinctive role in hematopoiesis.

The overall structure of the mitochondria of many cell types can change rapidly in response to different biological stimuli (Cervený et al., 2007), suggesting that mitochondrial dynamics are highly regulated. Sustained mitochondrial elongation induces senescence-associated phenotypic changes (Lee et al., 2007b). So too, during cardiomyocyte differentiation, mitochondria form long tubules (Chung et al., 2007). Formation of long tubules is highly relevant for mitochondrial function, because it improves mitochondrial transport and improves efficiency of energy transmission and Ca²⁺ dynamics between mitochondria. We found that mitochondrial length and the rigor of mitochondrial staining by the redox-sensitive dye correlated with *RBP2* levels. Consistent with the idea that mitochondria of filamentous structure may facilitate the delivery of membrane potential to specific subcellular regions (Skulachev, 2001), cells with *RBP2* knockdown showed widespread staining by this dye. Also, repression of *MFN2* is known to lead to a reduced mitochondrial membrane potential as well (Pich et al., 2005). Interestingly, the role of *MFN2* in mitochondrial energization is independent of its role in mitochondrial fusion. Therefore, *RBP2* may be directly involved in the negative control of mitochondrial fusion and energization, at least in part, by reducing mitofusin gene expression. Downregulation of *RBP2* triggers both processes that may contribute to “flat” cell phenotype in SAOS-2 cells, consistent with data on rat *MFN2* protein, which functions as a cell proliferation suppressor (Chen et al., 2004). *RBP2* proteins are conserved from fungi to human. We propose that regulation of enzymes and ribosomes present in mitochondria by *RBP2* is an ancient event in evolution. For free-living, single-celled organisms the critical criterion in the decision to divide in a given condition is nutrient supply. In yeast in response to hundreds of various growth conditions, the group of genes that behave in a coregulated manner encode mitochondrial proteins (Hughes et al., 2000). In complex organisms, extracellular signals, such as growth factors and antimetabolites, determine tissue- and cell-specific gene expression. Gene expression data analysis of *RB*^{-/-} cells with reintroduced pRB function or with reduced *RBP2* function showed an overrepresentation of genes encoding cell surface and cell adhesion molecules, receptors, and molecules with growth factor activity. Thus, *RBP2* inactivation leads, still in an unknown manner, to the increased expression of genes involved in development and in extracellular regulation (Figure 6). Our combined analysis sheds light on the mechanisms of the differentiation transcriptional switch mediated by *RBP2* and provides a framework for studies on the contribution of the pRB/*RBP2* pathway to disease pathogenesis such as in leukemia.

EXPERIMENTAL PROCEDURES

Cell Culture and Transfections

The plasmid pcDNA3-HA-*RBP2*mut was generated by replacing H483 and E485, involved in Fe(II) binding, with alanines. The plasmid pBabe-Puro-HA-RB(LP) was used to overexpress the large pocket of pRB. For knockdown experiments, we used *RBP2* siRNA duplex sequences No.4 and its control 4sc (Benevolenskaya et al., 2005) and *MFN2* siRNA duplex 5'-GGCUUUCAAGUGAGGAUGUTT-3' (Sigma).

ChIP-on-Chip, ChIP, and Gene Expression Profiling Analyses

For ChIP-on-Chip we used a self-printed array containing PCR-generated probes representing the proximal promoter regions of approximately 19K human genes. The probes were designed to span approximately 1 kb of promoter region between -500 bp and +500 bp of the transcription start site. Chromatin immunoprecipitation, amplification, hybridization to array, and processing of data were performed as described for the previous version of human 13K array (Odom et al., 2004). Comparison of the affinity-purified rabbit RBP2 antibodies 1416 and 2411 (Benevolenskaya et al., 2005) in the location analysis in U937 cells showed that they produce similar data sets. Anti-H3K4me3 (ab8580) and anti-total H3 (ab1791) were from Abcam. A whole-chip error model was used to calculate confidence values (p values) for each spot on the array, which indicated the significance of enrichment for each DNA species on the array. Each experiment was performed in triplicate. For gene expression analysis, we used a self-printed array of the Operon Biotechnologies Human 35K oligo set (release 3.0.3, <http://www.operon.com/>) for profiling of U937 cells, and the Affymetrix HG-U133A2.0 array for SAOS-2 cells. Total RNA was isolated from cells in triplicate.

Statistical Analysis

Functional annotation of genes based on Gene Ontology (Consortium, 2006) were extracted from Ensembl v.42 (Hubbard et al., 2007). Note that GO terms are organized into structures called directed acyclic graphs (DAGs), such that a specialized term can be associated with several less specialized terms. We used an inclusive analysis, in which genes annotated with terms that are descendant of the term corresponding to the level chosen take the annotation from the parent.

Z-score analysis: $Z_x = (X - \mu_x) / \sigma_{\bar{x}}$ (where μ_x = mean, $\sigma_{\bar{x}}$ = standard error). $\sigma_{\bar{x}}$ was calculated as $\sigma_{\bar{x}} = \sqrt{p(1-p)/N}$ (where p = proportion of genes in the category in question that are RBP2 targets or have expression fold change > 2 and N = number of genes in the category). Significance levels were corrected for multiple comparisons in accordance with False Discovery Rate (Benjamini and Hochbert, 1995). p values were estimated from Z-score using the algorithm described (Ibbetson, 1963). Tissue expression data were obtained from GNF Gene Atlas v.2 (Su et al., 2004). A gene is considered to be preferentially expressed in a particular tissue if the Affymetrix value in this tissue is twice the median of all tissues for this gene. TFBS in promoter sequences (1 kb upstream transcription start site) were predicted with Match algorithm using position weight matrices from TRANSFAC database v. 8.4 (Matys et al., 2003). Enrichment of TFBS in RBP2 target genes was analyzed with Chi square statistics.

Flow Cytometry and Fluorescent Microscopy

BrdU content and expression of CD11b were quantified by flow cytometry by using an indirect immunofluorescence staining technique. Cells were labeled with propidium iodide and treated with anti-BrdU (Becton Dickinson) or antihuman CD11b (ICRF44 BD Biosciences) monoclonal antibodies. Cells were analyzed for size and granularity and the percentage of CD11b-positive low granular cells was determined. All samples were analyzed by Beckman-Coulter Epics Elite ESP flow cytometer and the Elite V.4.02 software. The phase distribution of cell cycle was determined by "Multicycle AV" (Phoenix Flow Systems). COX4 rabbit antibody (ab16056, Abcam) was used as a mitochondrial marker, and anti-HA 12CA5 hybridoma supernatant was used for detection of HA-tagged proteins. Live cells were labeled with RedoxSensor red CC-1 (Molecular Probes). Cells were observed using fluorescent microscopy (Zeiss Axioplan2), and images were acquired using AxioVision Version 4.1 software.

Supplementary Material

Refer to Web version on PubMed Central for supplementary material.

Acknowledgments

We thank W.G. Kaelin for stimulating discussions throughout this work and for critical reading of the manuscript; S.J. Furney, A. Bigas and M. Alba for valuable comments; and M. Beshiri for technical assistance. This project has been funded with grants #05-40 and 07-13 from the American Cancer Society, Illinois Division, #0850172Z from the American Heart Association (E.V.B.), and it was partially supported by the 5RO1-CA076120-09 (PI: W.G. Kaelin, Jr.) while being in W.G. Kaelin's lab. N.L.-B. is a recipient of a Ramón y Cajal contract of the Spanish Ministry of Science and Education (MEC) and acknowledges funding from the International Human Frontier Science Program Organization (HFSPO) and the MEC grant number SAF2006-0459.

REFERENCES

- Balciunaite E, Spektor A, Lents NH, Cam H, Te Riele H, Scime A, Rudnicki MA, Young R, Dynlacht BD. Pocket protein complexes are recruited to distinct targets in quiescent and proliferating cells. *Mol. Cell. Biol* 2005;25:8166–8178. [PubMed: 16135806]
- Benevolenskaya EV. Histone H3K4 demethylases are essential in development and differentiation. *Biochem. Cell Biol* 2007;85:435–443. [PubMed: 17713579]
- Benevolenskaya EV, Murray HL, Branton P, Young RA, Kaelin WG Jr. Binding of pRB to the PHD protein RBP2 promotes cellular differentiation. *Mol. Cell* 2005;18:623–635. [PubMed: 15949438]
- Benjamini Y, Hochbert Y. Controlling the false discovery rate: A practical and powerful approach to multiple testing. *Journal of the Royal Statistical Society. Series B (Methodological)* 1995;57:289–300.
- Bergh G, Ehinger M, Olofsson T, Baldetorp B, Johnsson E, Brycke H, Lindgren G, Olsson I, Gullberg U. Altered expression of the retinoblastoma tumor-suppressor gene in leukemic cell lines inhibits induction of differentiation but not G1-accumulation. *Blood* 1997;89:2938–2950. [PubMed: 9108414]
- Bernstein BE, Humphrey EL, Erlich RL, Schneider R, Bouman P, Liu JS, Kouzarides T, Schreiber SL. Methylation of histone H3 Lys 4 in coding regions of active genes. *Proc. Natl. Acad. Sci. USA* 2002;99:8695–8700. [PubMed: 12060701]
- Bernstein BE, Meissner A, Lander ES. The mammalian epigenome. *Cell* 2007;128:669–681. [PubMed: 17320505]
- Boyer LA, Lee TI, Cole MF, Johnstone SE, Levine SS, Zucker JP, Guenther MG, Kumar RM, Murray HL, Jenner RG, et al. Core transcriptional regulatory circuitry in human embryonic stem cells. *Cell* 2005;122:947–956. [PubMed: 16153702]
- Calvo S, Jain M, Xie X, Sheth SA, Chang B, Goldberger OA, Spinazzola A, Zeviani M, Carr SA, Mootha VK. Systematic identification of human mitochondrial disease genes through integrative genomics. *Nat. Genet* 2006;38:576–582. [PubMed: 16582907]
- Cerveny KL, Tamura Y, Zhang Z, Jensen RE, Sesaki H. Regulation of mitochondrial fusion and division. *Trends Cell Biol* 2007;17:563–569. [PubMed: 17959383]
- Chen H, Detmer SA, Ewald AJ, Griffin EE, Fraser SE, Chan DC. Mitofusins Mfn1 and Mfn2 coordinately regulate mitochondrial fusion and are essential for embryonic development. *J. Cell Biol* 2003;160:189–200. [PubMed: 12527753]
- Chen KH, Guo X, Ma D, Guo Y, Li Q, Yang D, Li P, Qiu X, Wen S, Xiao RP, Tang J. Dysregulation of HSG triggers vascular proliferative disorders. *Nat. Cell Biol* 2004;6:872–883. [PubMed: 15322553]
- Christensen J, Agger K, Cloos PA, Pasini D, Rose S, Sennels L, Rappsilber J, Hansen KH, Salcini AE, Helin K. RBP2 belongs to a family of demethylases, specific for tri- and dimethylated lysine 4 on histone 3. *Cell* 2007;128:1063–1076. [PubMed: 17320161]
- Chung S, Dzeja PP, Faustino RS, Perez-Terzic C, Behfar A, Terzic A. Mitochondrial oxidative metabolism is required for the cardiac differentiation of stem cells. *Nat. Clin. Pract. Cardiovasc. Med* 2007;4 Suppl 1:S60–S67. [PubMed: 17230217]

- Cloos PA, Christensen J, Agger K, Helin K. Erasing the methyl mark: histone demethylases at the center of cellular differentiation and disease. *Genes Dev* 2008;22:1115–1140. [PubMed: 18451103]
- Consortium GO. The Gene Ontology (GO) project in 2006. *Nucleic Acids Res* 2006;34:D322–D326. [PubMed: 16381878]
- Dey BK, Stalker L, Schnerch A, Bhatia M, Taylor-Papdimetriou J, Wynder C. The histone demethylase KDM5b/JARID1b plays a role in cell fate decisions by blocking terminal differentiation. *Mol. Cell Biol.* 2008 Published online June 30, 2008. 10.1128/MCB.00128-08.
- Dimova DK, Dyson NJ. The E2F transcriptional network: old acquaintances with new faces. *Oncogene* 2005;24:2810–2826. [PubMed: 15838517]
- Fattaey AR, Helin K, Dembski MS, Dyson N, Harlow E, Vuocolo GA, Hanobik MG, Haskell KM, Oliff A, Defeo-Jones D. Characterization of the retinoblastoma binding proteins RBP1 and RBP2. *Oncogene* 1993;8:3149–3156. [PubMed: 8414517]
- Guenther MG, Levine SS, Boyer LA, Jaenisch R, Young RA. A chromatin landmark and transcription initiation at most promoters in human cells. *Cell* 2007;130:77–88. [PubMed: 17632057]
- Hollenhorst PC, Shah AA, Hopkins C, Graves BJ. Genome-wide analyses reveal properties of redundant and specific promoter occupancy within the ETS gene family. *Genes Dev* 2007;21:1882–1894. [PubMed: 17652178]
- Hubbard TJ, Aken BL, Beal K, Ballester B, Caccamo M, Chen Y, Clarke L, Coates G, Cunningham F, Cutts T, et al. Ensembl 2007. *Nucleic Acids Res* 2007;35:D610–D617. [PubMed: 17148474]
- Hughes TR, Marton MJ, Jones AR, Roberts CJ, Stoughton R, Armour CD, Bennett HA, Coffey E, Dai H, He YD, et al. Functional discovery via a compendium of expression profiles. *Cell* 2000;102:109–126. [PubMed: 10929718]
- Ibbetson D. Algorithm 209. *Gauss. Commun. ACM* 1963;6:616.
- Iwase S, Lan F, Bayliss P, de la Torre-Ubieta L, Huarte M, Qi HH, Whetstine JR, Bonni A, Roberts TM, Shi Y. The X-linked mental retardation gene SMCX/JARID1C defines a family of histone H3 lysine 4 demethylases. *Cell* 2007;128:1077–1088. [PubMed: 17320160]
- Kim YW, Otterson GA, Kratzke RA, Coxon AB, Kaye FJ. Differential specificity for binding of retinoblastoma binding protein 2 to RB, p107, and TATA-binding protein. *Mol. Cell. Biol* 1994;14:7256–7264. [PubMed: 7935440]
- Klose RJ, Yan Q, Tothova Z, Yamane K, Erdjument-Bromage H, Tempst P, Gilliland DG, Zhang Y, Kaelin WG Jr. The retinoblastoma binding protein RBP2 is an H3K4 demethylase. *Cell* 2007;128:889–900. [PubMed: 17320163]
- Lee MG, Norman J, Shilatifard A, Shiekhhattar R. Physical and functional association of a trimethyl H3K4 demethylase and Ring6a/MBLR, a polycomb-like protein. *Cell* 2007a;128:877–887. [PubMed: 17320162]
- Lee S, Jeong SY, Lim WC, Kim S, Park YY, Sun X, Youle RJ, Cho H. Mitochondrial fission and fusion mediators, hFis1 and OPA1, modulate cellular senescence. *J. Biol. Chem* 2007b; 282:22977–22983. [PubMed: 17545159]
- Mao S, Neale GA, Goorha RM. T-cell oncogene rhombotin-2 interacts with retinoblastoma-binding protein 2. *Oncogene* 1997;14:1531–1539. [PubMed: 9129143]
- Matys V, Fricke E, Geffers R, Gossling E, Haubrock M, Hehl R, Hornischer K, Karas D, Kel AE, Kel-Margoulis OV, et al. TRANSFAC: transcriptional regulation, from patterns to profiles. *Nucleic Acids Res* 2003;31:374–378. [PubMed: 12520026]
- Mikkelsen TS, Ku M, Jaffe DB, Issac B, Lieberman E, Giannoukos G, Alvarez P, Brockman W, Kim TK, Koche RP, et al. Genome-wide maps of chromatin state in pluripotent and lineage-committed cells. *Nature* 2007;448:553–560. [PubMed: 17603471]
- Mootha VK, Bunkenborg J, Olsen JV, Hjerrild M, Wisniewski JR, Stahl E, Bolouri MS, Ray HN, Sihag S, Kamal M, et al. Integrated analysis of protein composition, tissue diversity, and gene regulation in mouse mitochondria. *Cell* 2003;115:629–640. [PubMed: 14651853]
- Odom DT, Zizlsperger N, Gordon DB, Bell GW, Rinaldi NJ, Murray HL, Volkert TL, Schreiber J, Rolfe PA, Gifford DK, et al. Control of pancreas and liver gene expression by HNF transcription factors. *Science* 2004;303:1378–1381. [PubMed: 14988562]

- Pich S, Bach D, Briones P, Liesa M, Camps M, Testar X, Palacin M, Zorzano A. The Charcot-Marie-Tooth type 2A gene product, Mfn2, up-regulates fuel oxidation through expression of OXPHOS system. *Hum. Mol. Genet* 2005;14:1405–1415. [PubMed: 15829499]
- Rojo M, Legros F, Chateau D, Lombes A. Membrane topology and mitochondrial targeting of mitofusins, ubiquitous mammalian homologs of the transmembrane GTPase Fzo. *J. Cell Sci* 2002;115:1663–1674. [PubMed: 11950885]
- Rovera G, O'Brien TG, Diamond L. Induction of differentiation in human promyelocytic leukemia cells by tumor promoters. *Science* 1979;204:868–870. [PubMed: 286421]
- Skulachev VP. Mitochondrial filaments and clusters as intracellular power-transmitting cables. *Trends Biochem. Sci* 2001;26:23–29. [PubMed: 11165513]
- Su AI, Wiltshire T, Batalov S, Lapp H, Ching KA, Block D, Zhang J, Soden R, Hayakawa M, Kreiman G, et al. A gene atlas of the mouse and human protein-encoding transcriptomes. *Proc. Natl. Acad. Sci. USA* 2004;101:6062–6067. [PubMed: 15075390]
- Tan K, Shaw AL, Madsen B, Jensen K, Taylor-Papadimitriou J, Freemont PS. Human PLU-1 Has transcriptional repression properties and interacts with the developmental transcription factors BF-1 and PAX9. *J. Biol. Chem* 2003;278:20507–20513. [PubMed: 12657635]
- Taverna SD, Li H, Ruthenburg AJ, Allis CD, Patel DJ. How chromatin-binding modules interpret histone modifications: lessons from professional pocket pickers. *Nat. Struct. Mol. Biol* 2007;14:1025–1040. [PubMed: 17984965]
- Tu S, Teng YC, Yuan C, Wu YT, Chan MY, Cheng AN, Lin PH, Juan LJ, Tsai MD. The ARID domain of the H3K4 demethylase RBP2 binds to a DNA CCGCCC motif. *Nat. Struct. Mol. Biol* 2008;15:419–421. [PubMed: 18270511]
- van Zutven LJ, Onen E, Velthuisen SC, van Drunen E, von Bergh AR, van den Heuvel-Eibrink MM, Veronese A, Mecucci C, Negrini M, de Greef GE, Beverloo HB. Identification of NUP98 abnormalities in acute leukemia: JARID1A (12p13) as a new partner gene. *Genes Chromosomes Cancer* 2006;45:437–446. [PubMed: 16419055]
- Whitfield ML, Sherlock G, Saldanha AJ, Murray JI, Ball CA, Alexander KE, Matese JC, Perou CM, Hurt MM, Brown PO, Botstein D. Identification of genes periodically expressed in the human cell cycle and their expression in tumors. *Mol. Biol. Cell* 2002;13:1977–2000. [PubMed: 12058064]

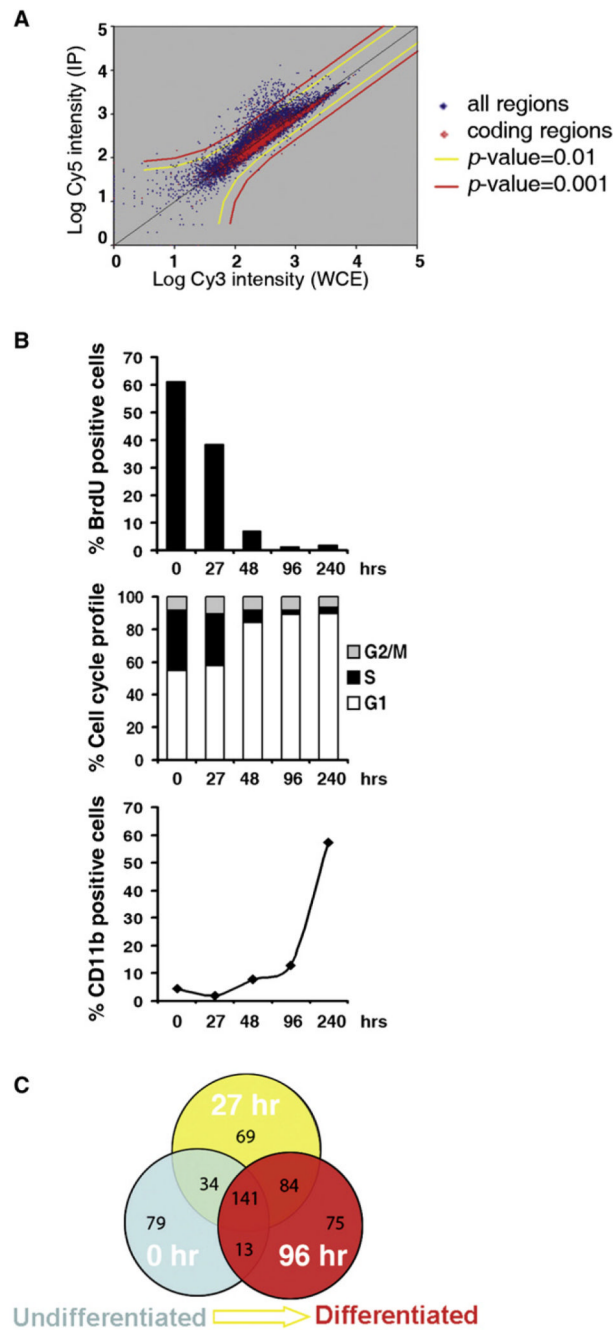


Figure 1. RBP2 Location Analysis Data

(A) Location analysis scatter plot. DNA fragments derived from ChIP were labeled with Cy5 and compared to genomic DNA fragments that were not enriched through immunoprecipitation and were labeled with Cy3. Both samples were hybridized to a single array. Representative scatter plot for RBP2 includes a presentation with coding regions highlighted in red.

(B) Characterization of proliferation and differentiation of U937 cells under the TPA treatment condition used in the study. Cells were labeled with propidium iodide and BrdU and analyzed by flow cytometry to count proliferating cells and the distribution of cells in the various phases of the cell cycle. Expression of differentiation marker CD11b was

determined by flow cytometry. The cells become growth arrested and increase expression of CD11b, which indicates that they have become differentiated monocytes.

(C) Venn diagram of genome-wide RBP2 binding during differentiation progression. Circle represents the number of RBP2 target sequences, with p value < 0.002, in certain conditions. Data for cells in three conditions are shown in different colors.

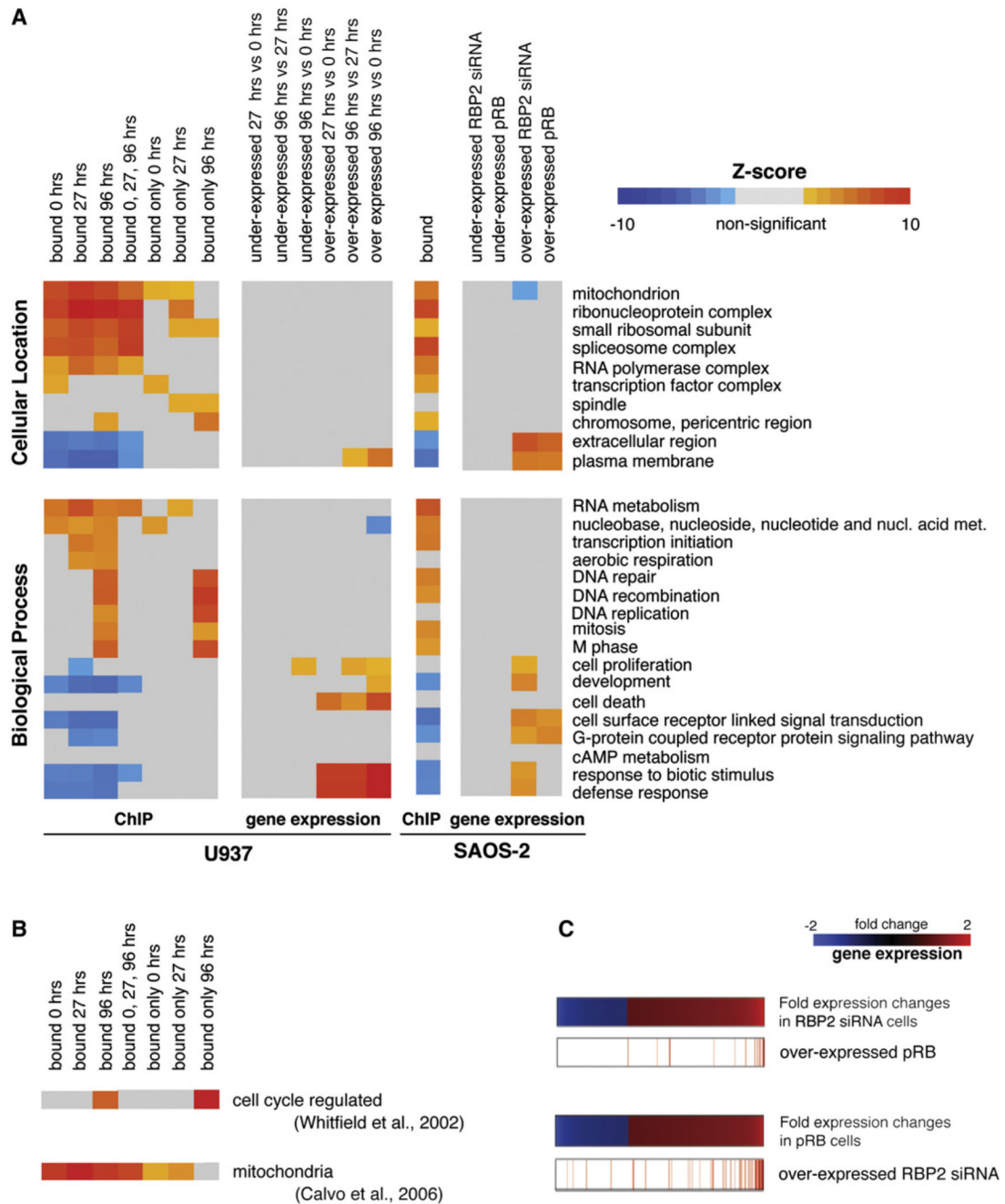


Figure 2. Functional Analysis of RBP2 Target Genes and Differentially Expressed Genes

(A) Target genes for RBP2 and differentially expressed genes in U937 and SAOS-2 cells were analyzed for enrichment of Gene Ontology terms using Z-score statistics. This test measures if in a set of genes, i.e., RBP2 target genes specific for 96 hr (“bound only 96 hrs”), the proportion of genes with a particular GO term differs statistically from random expectations. Positive Z-score values indicate that there is an enrichment of this term in the set of genes analyzed. Negative Z-scores indicate underrepresentation. Z-scores are shown in a color code scale; colors toward red signify enrichment for a particular GO term. Colors toward blue signify underrepresentation of a GO term. Gray means no statistically significant difference.

(B) Enrichment analysis, using Z-score statistics, of cell-cycle-regulated genes and genes encoding components of the mitochondrion.

(C) Overlap between genes differentially expressed in $RB^{-/-}$ SAOS-2 cells depleted for RBP2 (RBP2 siRNA) and after reintroduction of pRB (pRB). Genes overexpressed in pRB cells are shown in red lines in the ordered position according to its fold change expression in RBP2 siRNA cells. Similarly, genes overexpressed in RBP2 siRNA cells are shown in their ordered position according to the expression fold change in pRB cells. These panels show a high degree of overlap between genes overexpressed in RBP2 siRNA cells and pRB cells.

The figure consists of several tables and a legend. The top table is a 2x2 contingency table for H3K4me3 enrichment. Below it are two columns of 2x2 contingency tables for TFBS enrichment, one for predicted TFBS and one for experimentally validated TFBS. A legend at the bottom indicates that red boxes highlight family members of E2F- and ETS-responsive elements.

| Enrichment of H3K4me3 | |
|-----------------------|-------|
| Category | Count |
| Enriched | 100 |
| Not Enriched | 50 |
| Total | 150 |

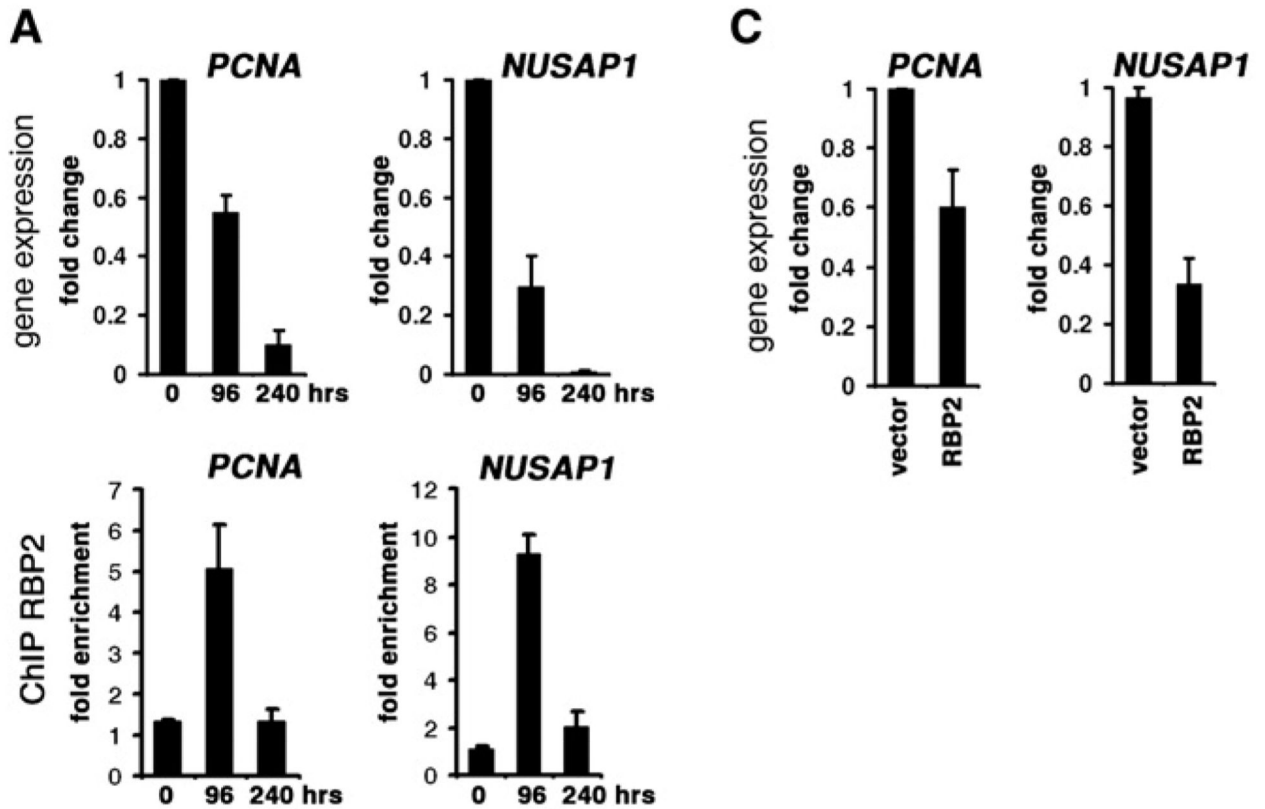
| Predicted Transcription Factor Binding Sites (TFBS) | |
|---|-------|
| Category | Count |
| Enriched | 100 |
| Not Enriched | 50 |
| Total | 150 |

| Experimentally Validated Transcription Factor Binding Sites (TFBS) | |
|--|-------|
| Category | Count |
| Enriched | 100 |
| Not Enriched | 50 |
| Total | 150 |

Legend: Red box encapsulates family members of E2F- and ETS-responsive elements.

Figure 3. RBP2 Colocalizes with H3K4 Trimethylated Nucleosomes and a Number of Transcription Factors

Statistics analysis (Chi square test) of the enrichment of H3K4me3 at the promoters of RBP2 target genes is on the top. Statistics analysis (Chi square test) of the enrichment of predicted transcription factor binding sites (TFBS) in RBP2 target promoters and enrichment of RBP2 target genes among E2F4, p107, and p130 experimentally validated target genes is below. Red box encapsulates family members of E2F- and ETS-responsive elements.

**B**

| | RBP2 target only at 96 hrs | | all |
|--------------------------------------|----------------------------|--------|-------------|
| | p (n) | pvalue | p (n) |
| negative fold change 96 vs 27 hrs | 0.52 (33) | 0.009 | 0.37 (9731) |

* pvalue from chi square analysis

p = proportion of genes

n = number of genes

Figure 4. RBP2 Is Recruited to Highly Active Genes to Mediate Repression Accompanying Differentiation

(A) Expression analysis and ChIP assays using RBP2 antibodies of cell-cycle genes in U937 cells. "0," "96," and "240" are hours after TPA addition. The same samples used in the real-time RT-PCR (qRT-PCR) were used in gene expression profiling experiments. The ChIP results were normalized to the levels of the intergenic region 20D bound.

(B) A significant number of RBP2 target genes specific for 96 hr show lower values of expression at 96 hr compared to 27 hr (negative fold change). The table shows the results for the chi square test (p value = 0.009).

(C) Expression levels of cell-cycle genes after overexpression of RBP2. U937 cells were treated with TPA for 96 hr after nucleofection with a RBP2 expression plasmid, and expression levels were determined by qRT-PCR. The bars indicate mean values and are presented with standard errors for three independent experiments. The qRT-PCR data were normalized to the levels of *beta-2-microglobulin* (*B2M*).

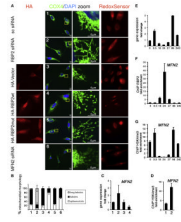


Figure 5. RBP2 Affects Mitochondrial Morphology through H3K4me3 Demethylation

(A) Fluorescent images of SAOS-2 cells transfected with the siRNAs to RBP2 (RBP2 siRNA), MFN2 (MFN2 siRNA), or scrambled version of RBP2 siRNA (sc siRNA), as well as with expression plasmids that encode HA tag (HA-Vector), HA-tagged RBP2 (HA-RBP2wt) or RBP2 mutant (HA-RBP2mut). Cells were selected for transfected cells and either fixed and immunostained for HA and the mitochondrial marker COX4 or labeled with the stain for redox potential. The cells were counterstained with DAPI to visualize cell nuclei. The images are marked from 1 to 6 and are representative of three independent experiments. The scale bar is 5 μ m.

(B) Quantification of mitochondrial classes in cells from the experiments in (A).

Quantification was performed for the experiments 1 to 6 in (A). Mitochondria were visualized by COX4 immunostaining in about 200 cells for each transfection. Cells with mitochondria extending at more than 5 μ m were counted as “long tubule” cells; cells with shorter mitochondria were considered as either “tubule” or “sphere/rod” cells. The results are presented as the percentage of cells belonging to each of three morphological classifications. The bars indicate means of three independent experiments with standard errors.

(C) Expression levels of *MFN2* in cells prepared in parallel with cells (from 1 to 4) in (A). The bars indicate mean values and are presented with standard errors for two experiments.

(D) ChIP analysis of *MFN2* promoter using H3K4me3-specific antibodies in SAOS-2 cells transfected with RBP2 or scrambled siRNA (1 and 2 as in [A]). The results are presented as enrichment in *MFN2* promoter relative to the intergenic region 26E; mean values and standard errors are from two independent experiments.

(E) Expression analysis of *MFN2* in U937 cells treated with TPA. Triplicate qRT-PCR reactions were assayed to generate mean with standard error and were reproducible in two independent experiments. Time points with the most robust *MFN2* gene expression changes are presented; see Figure S9 for a detailed gene expression profile.

(F) ChIP analysis of *MFN2* promoter using RBP2 antibodies.

(G) ChIP analysis of *MFN2* promoter using H3K4me3-specific antibodies.

The bars in (F) and (G) indicate mean values and are presented with standard errors for three independent experiments. The normalization in (C) and (E)–(G) is as in Figure 4.

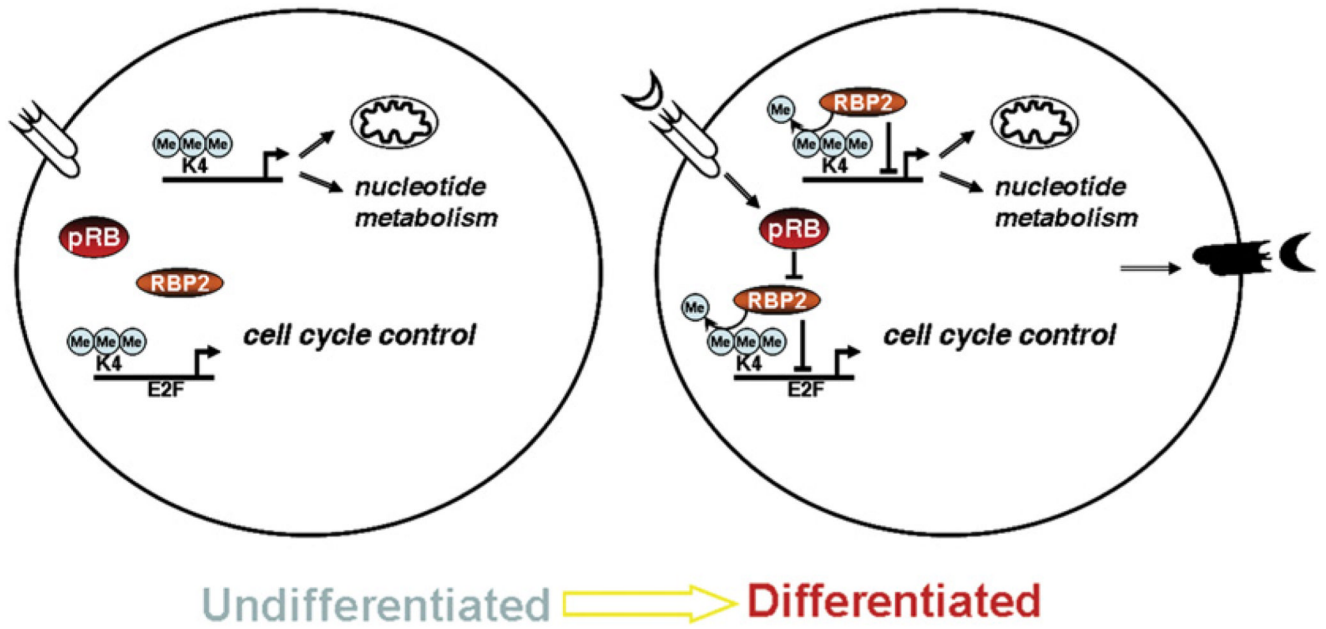


Figure 6. RBP2 Regulatory Circuit

RBP2 can occupy promoters of genes involved in mitochondrial function, nucleotide metabolism, and cell cycle. An extrinsic signal informs the cell about external conditions, and this leads toward differentiation through pRB-dependent transmission down to RBP2. It initiates recruitment of RBP2 to genes and their repression. All together, this results in the expression of extracellular proteins that can inform neighboring cells about continuous differentiation.